Type of the Paper (Article)

Aromatic polyimide membranes with *tert*-butyl and carboxylic side groups for gas separation applications. Covalent crosslinking study

Noelia Esteban[1], Marta Juan y Seva[2], Carla Aguilar-Lugo[3], Jesús A. Miguel[1], Claudia Staudt[4] ,José G. de la Campa[2], Cristina Álvarez[2,5,*], Ángel E. Lozano[1,2,5,*]

[1]IU CINQUIMA, University of Valladolid, Paseo Belén 5, E-47011 Valladolid, Spain.
[2]Institute of Polymer Science and Technology, ICTP-CSIC, Juan de la Cierva 3, E- 28006 Madrid, Spain.
[3]Materials Research Institute, National Autonomous University of Mexico, University City, 04510 Mexico City, Mexico
[4]Global Product and System Development Personal Care, BASF, 40789 Monheim, Germany
[5]SMAP, UA-UVA_CSIC, Associated Research Unit to CSIC. University of Valladolid, School of Sciences, Paseo Belén 7, E-47011 Valladolid, Spain.
*Corresponding authors: Cristina Álvarez; **cristina.alvarez@ictp.csic.es** and Angel E. Lozano; **lozano@ictp.csic.es**

Abstract: A set of aromatic copolyimides was obtained by reaction of 4,4′-(hexafluoroisopropylidene) diphthalic anhydride (6FDA), and mixtures of the diamines 1,4-bis(4-amino-2-trifluoromethylphenoxy)-2,5-di-*tert*-butylbenzene (CF_3TBAPB) and 3,5-diamino benzoic acid (DABA). These polymers were characterized and compared with the homopolymer derived from 6FDA and CF_3TBAPB. All copolyimides showed high molecular weight values and good mechanical properties. The presence of carboxylic groups in these copolymers allowed their cross-linking by reaction with 1,4-butanediol. The crosslinked polymer films were extensively characterized and it was observed that the degree of crosslinking was low in the copolyimides possessing a small number of carboxyl groups. The degradation temperature of these crosslinked copolyimides was lower than their corresponding non-crosslinked ones. Glass transition temperatures were higher than 260 °C, showing the non-crosslinked copolyimides the highest values. Young moduli of these crosslinked showed values higher than 1.9 GPa, and slightly lower elongation at break when compared with the precursor copolyimides. All copolyimides (precursor, and crosslinked ones) films could be tested as gas separation membranes. It was seen that CO_2 permeability values were around 100 barrer, having better selectivity than that of the homopolymer. Moreover, the plasticization resistance of the crosslinked material having a large number of carboxylic groups was excellent.

Keywords: aromatic polyimides, crosslinking, plasticization resistance, gas separation

1. Introduction

Although there are currently a large number of glassy polymeric materials that have excellent productivity to separate gas at high pressures [1], these materials, however, show some drawbacks due to the physical aging process, and the tendency to undergo plasticization processes when certain gas passes through the membrane [2–4].

The problem of plasticization in membranes occurs when these materials are subjected to high pressures in the presence of highly soluble gases in the polymeric matrix, such as carbon dioxide and hydrocarbons C≤3. Plasticization is the process by which an increase in the free volume of the polymer is produced, as well as an increase in the segmental mobility of the chains, due to their interaction with these soluble gases [5]. As a consequence of this process, the permeability of the membrane increases while its selectivity decreases, which leads to a very marked deterioration of its properties as a gas separation material [6].

Preprints (www.preprints.org) | NOT PEER-REVIEWED | Posted: 16 November 2022 doi:10.20944/preprints202211.0309.v1

Plasticization produces serious problems in the application of these materials at the industrial level. Thus, for example, natural gas consists mostly of CH_4 and variable fractions of heavy gaseous hydrocarbons (ethane, propane, and butane, among others) and gases such as N_2 and CO_2, as well as traces of many other aromatic and paraffinic compounds. Among these components, CO_2, ethane, propane, and butane have a very high capacity to plasticize the membranes [7–13]. Therefore, this phenomenon prevents the application of polymeric membranes in the high-pressure separation of CO_2 and hydrocarbons for natural gas purification [13,14]. Plasticization with other condensable gases also occurs in other processes that have high economic importance [15] such as ethene/ethane[16], propylene/propane [17,18], or butadiene/butane separations [19].

In particular, the CO_2-induced plasticization phenomenon results in a permeability minimum at a certain pressure (plasticization pressure), together with a time dependence of CO_2 permeability above the plasticization pressure and a marked decrease of CO_2 selectivity to other gases at elevated pressures [20–23]. In addition, plasticization depends on other aspects that affect the gas separation properties: time [5,24], pressure [25], temperature [26,27], and thickness of the tested films [28,29].

One of the most commonly used methods to avoid or decrease the plasticization process consists of crosslinking the polymer chains, which reduces their mobility and restricts the volume increase of the membrane due to the presence of condensable gases [30–33]. In addition, crosslinking produces improvements in the chemical stability of polymers [34,35], as has been described in different processes, not only in gas separation [30,36,37] but also in other separation processes such as pervaporation [38,39]. However, plasticization also occurs in crosslinked membranes, although at higher pressures (or longer exposure times). It should also be noted that on numerous occasions, crosslinking is accompanied by a decrease in permeability, which implies a decrease in productivity [11,40–42].

Figure 1 shows, as an example, the effect of plasticization in aromatic polyimides.

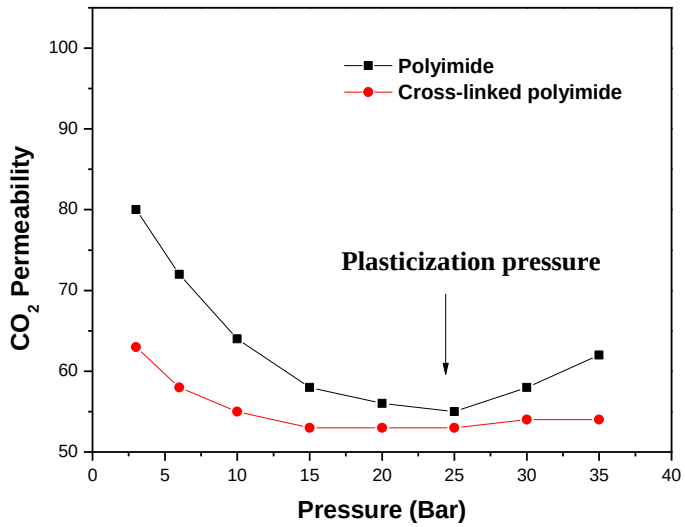

Figure 1. Example of plasticization in a linear and a crosslinked polyimide[4].

At least five types of generic crosslinking have been reported to reduce plasticization processes:

- Thermal crosslinking [33,43–45], where the materials are subjected to elevated temperatures, generally above 300 °C and sometimes up to values close to 400 °C, that is, at temperatures above the Tg, so that intermolecular reactions occur between various groups of the polymer chain. In this type of crosslinking it is difficult to know whether small degradations also occur due to the high temperatures used and/or the high residence times at these temperatures [44,46–49]. In fact, some researchers have used this partial

 doi:10.20944/preprints202211.0309.v1

degradation process as an advantage, since partially pyrolyzed membranes (PPMs), because removal of thermolabile groups, present in the macromolecular chain, translated in materials having good gas separation properties [50,51] However, this method has the disadvantage that a loss in mechanical properties was observed due to partial degradation of the macromolecular structure [47].

- Crosslinking of materials by ultraviolet (UV) irradiation [52,53]. This technique has been used to prevent plasticization at high pressures, although permeability is reduced.

- Formation of semi-interpenetrated networks (sIPNs). This methodology, which consists of crosslinking a polymer in the presence of another linear polymer, is very versatile and gives good results in some cases, but its main drawback is its high cost [25].

- Ionic crosslinking. This method uses polymers that have certain functional groups that react with polyvalent cations, such as aluminum acetylacetonate $Al(acac)_3$ [54]. However, this type of crosslinking has not been studied very exhaustively and there is no detailed characterization of these materials to date.

- Covalent crosslinking, which is the most commonly used method, where nucleophilic, di- or multifunctional reagents capable of reacting with electrophilic groups present in the polymer, are generally used. Numerous works have been reported in this regard, mainly using diamines [55–57] and diols [25,40] as crosslinking agents. The difunctional crosslinking compounds act as spacer agents between the chains, preventing the decrease in permeability from being as pronounced as in the previous methods [11,57].

Most of the works cited above are based on the study of copolymers derived from the 4,4′-(hexafluoroisopropylidene)diphtalic anhydride (6FDA), which have very interesting properties as gas separation membranes, although they have the drawback of being very susceptible to plasticization at high working pressures [58,59].

Likewise, the synthesis of copolyimides including 3,5-diamino benzoic acid (DABA), which has an acid group (-COOH) of high polarity, has been the subject of exhaustive study due to the great versatility of functionalization provided by the carboxylic group [31,60–63].

In this research, the synthesis of new copolymers derived from the reaction between the dianhydride 6FDA, and a mixture of the diamines; 1,4-bis(4-amino-2-trifluoromethylphenoxy)-2,5-di-*tert*-butylbenzene (CF_3TBAPB) and DABA diamines, have been carried out, has been carried out to improve the performance of their corresponding homopolymers as gas separation membranes.

Aromatic polyimides derived from the diamine (Figure 2) were synthesized and evaluated as gas separation materials by us and it was observed that the materials exhibited excellent properties [64,65]. In this work, the main objective has consisted of obtaining aromatic copolyimides derived from CF_3TBAPB and DABA, which will allow their chemical crosslinking, through the carboxyl groups present in the polymeric materials, bringing about an improvement in plasticization resistance.

Preprints (www.preprints.org) | NOT PEER-REVIEWED | Posted: 16 November 2022 doi:10.20944/preprints202211.0309.v1

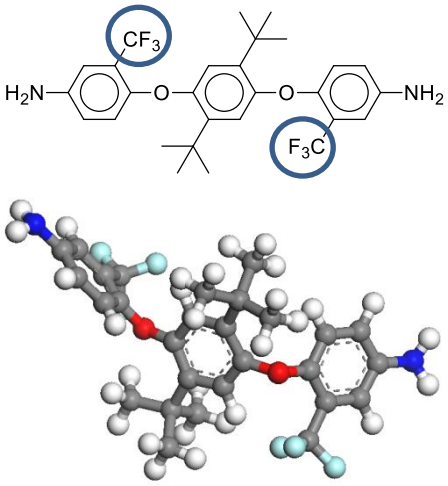

Figure 2. Structure of 4-bis(4-amino-2-trifluoromethylphenoxy)2,5-di-*tert*-butylbencene (CF_3TBAPB)

The introduction of carboxylic acids into the polymeric structure provides in some cases improvements in the balance of properties, although this improvement is not general because is highly dependent on the structure of the other diamine comonomer and also in the dianhydride used [59]. In general, it can be said that for most of the aromatic polyimides of comparable structure, lower permeabilities and higher selectivities are obtained when DABA is employed as a comonomer.

Subsequently, covalent crosslinking of the synthesized copolyimides was carried out and the gas properties were evaluated.

Finally, a study of plasticization at elevated pressures was carried out.

The chemical structure of the synthesized copolyimides, as well as the proportions of the diamines used, are shown in Figure 3.

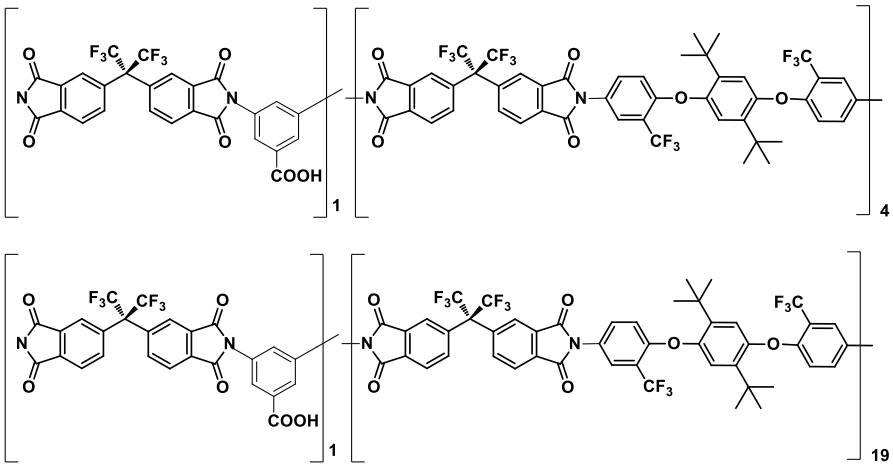

Figure 3. Chemical structure of the synthesized copolymers 6FDA-[DABA-CF_3TBAPB (1/4)] y 6FDA-[DABA-CF_3TBAPB (1/19)].

The proportions of DABA in the copolymer, and the amount of crosslinking agent used, were chosen based on the results obtained by Wind [55,66] and Staudt-Bickel [30,67]. In our study, 1,4-butanediol was selected as the crosslinking agent, since it is one of the diols that has given the best results in crosslinking reactions [30].

Figure 3 shows the crosslinking reaction scheme of a copolyimide incorporating DABA with a large excess of 1,4-butanediol. In the first stage, initial monoesterification

Preprints (www.preprints.org) | NOT PEER-REVIEWED | Posted: 16 November 2022 doi:10.20944/preprints202211.0309.v1

reactions occur, followed by subsequent esterification of the free OH group and subsequent crosslinking, directly or by transesterification processes.

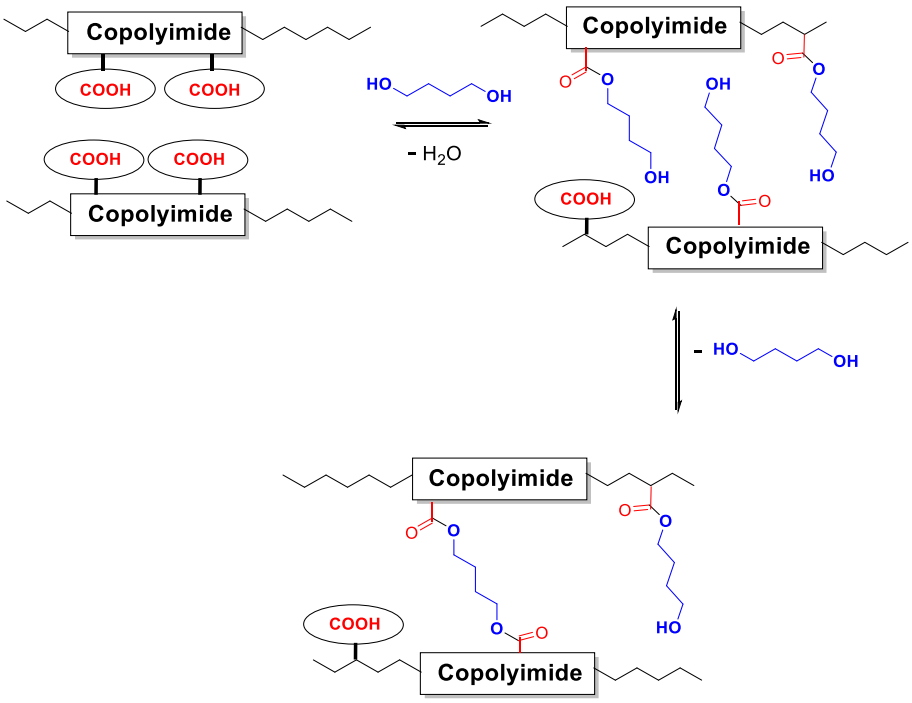

Figure 4. Scheme of covalent crosslinking reaction in a copolyimide incorporating DABA.

There is a probability that all the species indicated in Figure 4 (acid, monoester, and diester) coexist in the polymer material, although, since the diol reacts in large stoichiometric excess, it is assumed that the amount of free -COOH groups should be very small. However, the most likely species will be the monoester groups, which could not have undergone crosslinking in the absence of optimum conditions. Another aspect to take into account is that the use of a reagent excess makes it necessary to remove it from the material by prolonged washing, or by heat treatments above the glass transition temperature, Tg.

2. Materials and Methods

Anhydrous 1-methyl-2-pyrrolidone (NMP, Sigma-Aldrich), anhydrous pyridine (Py, Sigma-Aldrich), 4-dimethylaminopyridine (DMAP, Sigma-Aldrich), trimethylchlorosilane (TMSCl, Sigma-Aldrich), p-toluenesulfonic acid (Sigma-Aldrich), 1,4-butanediol (Sigma-Aldrich), and acetic anhydride (Sigma-Aldrich) together with other commercial solvents (chloroform, $CHCl_3$; N,N-dimethylacetamide; DMAc, tetrahydrofuran, THF, m-cresol) employed in this research, were obtained from commercial sources (Sigma-Aldrich) at their highest level of purity. Acetic anhydride was distilled before use.

3,5-diaminobenzoic acid DABASigma-Aldrich, > 97.5 %) diamine, and 4,4'-(hexafluoroisopropylidene)diphtalic anhydride (6FDA, TCI, >98 %) dianhydride, as well as the crosslinking agent 1,4-butanediol (Sigma-Aldrich), were obtained from commercial sources. 6FDA and DABA were purified by sublimation.

1,4-Bis(4-aminophenoxy)2,5-di-tert-butylbenzene (TBAPB) was synthesized by us in two steps, according to previously reported methods [64,65,68], from 2,5-di-tert-butylhydroquinone (Sigma-Aldrich, 99%) and p-chloronitrobenzene (Sigma-Aldrich, 99%) via nucleophilic aromatic substitution in the presence of potassium carbonate (K_2CO_3) (Panreac) and DMF (Sigma-Aldrich, 99.5%) as solvent, followed by catalytic reduction with hydrazine hydrate (Sigma-Aldrich, XX%) and Pd/C (Sigma-Aldrich, 10% Pd) as catalyst.

Preprints (www.preprints.org) | NOT PEER-REVIEWED | Posted: 16 November 2022 doi:10.20944/preprints202211.0309.v1

The 6FDA dianhydride was heated at 190 °C for 2 hours just before polymerization. Both polymerizations were carried out in DMAc and the cyclization was chemical, with acetic anhydride and pyridine.

2.1 Characterization methods

Monomers, polyimides, and copolyimides were characterized by attenuated total reflection Fourier transform infrared (ATR-FTIR), and ^{1}H (NMR) spectra in solution. These experiments were realized on a Bruker Advance 400 MHz spectrometer using DMSO-d_6 as solvent.

ATR-FTIR spectra of samples were measured using a Perkin Elmer RX-1 spectrometer with an ATR accessory.

Thermogravimetric analyses (TGA) were performed on a TA-Q500 analyzer heating the samples to 20 °C/min and using the Hi-Res (Thermal Analysis) method in the temperature range of 30 to 850 °C. Nitrogen was used as the purge gas (60 mL/min).

High-angle scattering patterns (WAXS) were recorded on a Bruker D8 Advance equipped with a Goebel mirror and a Vantec PSD, with CuK radiation (wavelenght = 1.54 Å), in a diffraction angle range between 3 and 60 °.

Solubility tests were done in a test tube where 1-2 mg of polymer and 1 mL of solvent were added. The system was subjected to magnetic agitation during 24 h. In case of not getting dissolved, it was heated at the boiling point of the solvent.

The density (ρ) of membranes was determined using a top-loading electronic XS105 Dual Range Mettler Toledo balance coupled with a density kit based on Archimedes' principle. The samples were sequentially weighed in air and into high-purity isooctane at room temperature. The density was calculated from Equation (1).

$$\rho = \rho_{\text{liquid}} \, x \, \frac{w_{air} - w_{liquid}}{w_{air}} \quad (1)$$

where ρ_{liquid} is the density of isooctane, w_{air} is the weight of the sample in air and w_{liquid} is its weight when submerged in isooctane. Four density measurements were made for each sample.

The density data were used to evaluate chain packing with the fractional free volume (FFV) calculated from the following Equation (2):

$$FFV = \frac{V_e - 1.3V_w}{V_e} \quad (2)$$

where V_e is the specific volume of the polymer and V_w is the polymer van der Waals volume calculated in the Biovia Materials Studio program[69]. A 20-unit polymer structure was built using the Builder Polymers and Atom Volumes and Surface algorithms of the program Materials Studio and was optimized by using the Compass force field to determine the molecular volume.

To measure the mechanical properties, strips 5 mm wide and 80 mm long were cut from polymer films and tested on an MTS Synergie-200 testing machine equipped with a 100 N load cell at room temperature. Pneumatic clamps were used, and an extension rate of 5 mm/min was applied with a gauge length of 10 mm.

Gas separation properties were measured in a barometric or constant volume apparatus using He, O_2, N_2, CO_2, and CH_4 with an upstream pressure of 3 bar and 35 °C of temperature. The membrane was maintained inside the barometric apparatus under a high vacuum for 12 h to remove possible traces of humidity.

Permeability values were obtained from the evolution of pressure of the downstream side. The permeability coefficient, P, was determined from the slope of the pressure vs. time curve under steady-state conditions where the relationship between permeate pressure and measurement time is linear. Before each experiment, the apparatus was vacuum-degassed. So, the membrane permeability can be obtained from the following equation:

Preprints (www.preprints.org) | NOT PEER-REVIEWED | Posted: 16 November 2022 doi:10.20944/preprints202211.0309.v1

$$P = \frac{273{,}15}{76} \times \frac{Vl}{\pi r^2 T p_o} \times \frac{dp}{dt} 10^{10} \quad (3)$$

where V is the volume of the lower chamber in cm^3, l is the thickness in cm of the membrane, T is the temperature in K, πr^2 is the effective area in cm^2 of the membrane, p_0 is the pressure in the upper chamber in bar, and dp/dt is the rate of the pressure rise under the steady state in mbar/s. The factors reference the results to standard pressure and temperature conditions (76 cmHg and 273.15 K).

The ideal selectivity between two gas species, A and B, is the ratio of the single gas permeabilities (Equation (4)).

$$\alpha_{A,B} = \frac{P_A}{P_B} \quad (4)$$

2.2 Synthesis of copolyimides and preparation of polymer films

Aromatic copolyimides with carboxyl groups were prepared by a two-step polycondensation reaction using the *in-situ* silylation of the diamine method [71,72] in the formation of the corresponding polyamic acid as explained below.

The synthetic method and conditions used for the synthesis of the COPOL-DABA(1/4) copolyimide are described below. The synthesis of the other copolymer, COPOL-DABA(1/19), was carried out in the same way but using the corresponding ratio of diamines (1/19).

In a three-necked flask, provided with mechanical stirring and N_2 stream, 7.0 mmol of both diamines (CF_3TBAPB: 5.6 mmol, 3.000 g; DABA: 1.4 mmol, 0.213 g) were dissolved in 10 mL of DMAc. Once dissolved, the solution was cooled to 0 °C, and TMSCl (14 mmol, 1.8 mL) and anhydrous pyridine (14 mmol, 1.2 mL) were added. The solution temperature was maintained for 5 min and then it was raised to room temperature to ensure the silylation of the diamine. Next, the temperature reaction was lowered again to 0 °C, and 7.0 mmol (3.100 g) of the 6FDA dianhydride together with DMAP (2.8 mmol, 0.342 g), and another 5 mL of DMAc were added. The reaction was stirred for about 16 h at room temperature, giving a viscous solution of polyamic acid.

Chemical cyclodehydration was carried out by the addition of an acetic anhydride/pyridine mixture (70 mmol/70 mmol). The mixture was stirred for 4 h at room temperature, heated at 40 °C for 1 h, and at 60 °C for a further 1 h (A coolant was attached at this stage to prevent evaporation of the reagents). After cooling to room temperature, the polymer solution was precipitated in water/ethanol (2/1) and washed sequentially several times with water and water/ethanol (2/1). The polymers were dried at 150 °C in an oven under vacuum for 16 h.

The polymer films were prepared by dissolving the polymers in DMAc at 5-6% wt/vol (w/v). Subsequently, the solutions were filtered with a 3.0 μm glass fiber Symta® filter and spread on a glass plate over a pre-leveled heating plate. For solvent removal, the films were heated for 16 h at 60 °C, and then the temperature was raised to 80 °C for 3 h more. Finally, the polymer film was heat treated as follows: 150 °C/24h/vacuum, 180 °C/30min/N_2, 200 °C/15 min/N_2, 200 ºC/15 min/vacuum, 250 °C/15 min/N_2, 280 °C/10 min/N_2.

2.3 Crosslinking by carboxylic group esterification

Crosslinking of the copolyimides in solid-state was performed as described in the literature, using 1,4-butanediol as the covalent crosslinking agent and p-toluenesulfonic acid as an acid catalyst[63].

Thus, a solution of copolymer (300 mg) in DMAc (10 mL) was prepared. Once dissolved, p-toluenesulfonic acid (3-5 mg per 1 g polymer) was added. After 30 min of stirring, 6 equivalents (per carboxyl group) of 1,4-butanediol were added and kept for 1 h more with stirring.

Preprints (www.preprints.org) | NOT PEER-REVIEWED | Posted: 16 November 2022 doi:10.20944/preprints202211.0309.v1

Subsequently, the membrane was obtained in the usual way. For solvent removal, the solution was heated for 16 h at 60 °C and then the temperature was raised to 80 °C for 3 h more. To achieve maximum crosslinking of the films, as well as the removal of unreacted compounds, the following heat treatment was carried out: 150 °C/24 h/vacuum and gradually raising the T to 280 °C/10 min/N_2.

Table 1 shows the designation to be used hereinafter, according to the proportion of diamines used.

Thus, in the copolyimides, here referred to as COPOL, the composition will be specified by (1/X), where 1 is the proportion of DABA and X is the proportion corresponding to CF_3TBAPB (X=4 or X=19). For the corresponding crosslinked films, COPOL-CCL (Covalent Cross-Linking) will be used. Finally, the generic term HOMOPOL will be used to refer to the polyimide 6FDA-CF_3TBAPB.

Table 1. Acronyms employed for the homopolymer, DABA-copolymers, and covalently crosslinked polymers.

Polymer	Acronym
6FDA-CF_3TBAPB	HOMOPOL
6FDA-[DABA-CF_3TBAPB (1/4)]	COPOL-DABA(1/4)
6FDA-[DABA-CF_3TBAPB (1/4)]*	COPOL-CCL(1/4)
6FDA-[DABA-CF_3TBAPB (1/19)]	COPOL-DABA(1/19)
6FDA-[DABA-CF_3TBAPB (1/19)]*	COPOL-CCL(1/19)

* Solid-state covalently crosslinked films with 1,4-butanediol

3. Results and Discussion

3.1 Synthesis of copolyimides. Preparation of crosslinked membranes.

The synthesis of copolyimides was carried out in the same way as described in the homopolymer synthesis section, adding a mixture of two diamines; DABA and CF_3TBAPB, and using the in situ silylation method, to form the corresponding copolymers. The cyclization was carried out chemically because this method produced polymer films with better mechanical properties.

The preparation of the crosslinked films has been described above. Concerning the final temperature of the heat treatment, to achieve maximum crosslinking, a temperature of 280 °C was chosen, based on the results published in the literature, which indicate that above that temperature decarboxylation and/or other types of crosslinking can occur, which would not allow the evaluation of the degree of transformation sought, and would produce partial degradation of the polymeric material.

3.2 Spectroscopic and structural characterization

3.2.1 NMR Spectroscopy

Figures 5 and 6 show the ^{1}H-NMR spectra in $CDCl_3$ of the synthesized copolyimides, COPOL-DABA(1/4) and COPOL-DABA(1/19) respectively. The proportions of DABA in the structure are relatively low, so no substantial changes were appreciated in the ^{13}C spectra.

The protons in *ortho* to the carboxylic group of the DABA diamine were observed (signal marked with a blue ellipse in the NMR spectra). The protons of the acid group were not observed under the conditions used in the experiment. These results agreed with others described previously for copolymers including the DABA monomer [50,59,73].

Preprints (www.preprints.org) | NOT PEER-REVIEWED | Posted: 16 November 2022 doi:10.20944/preprints202211.0309.v1

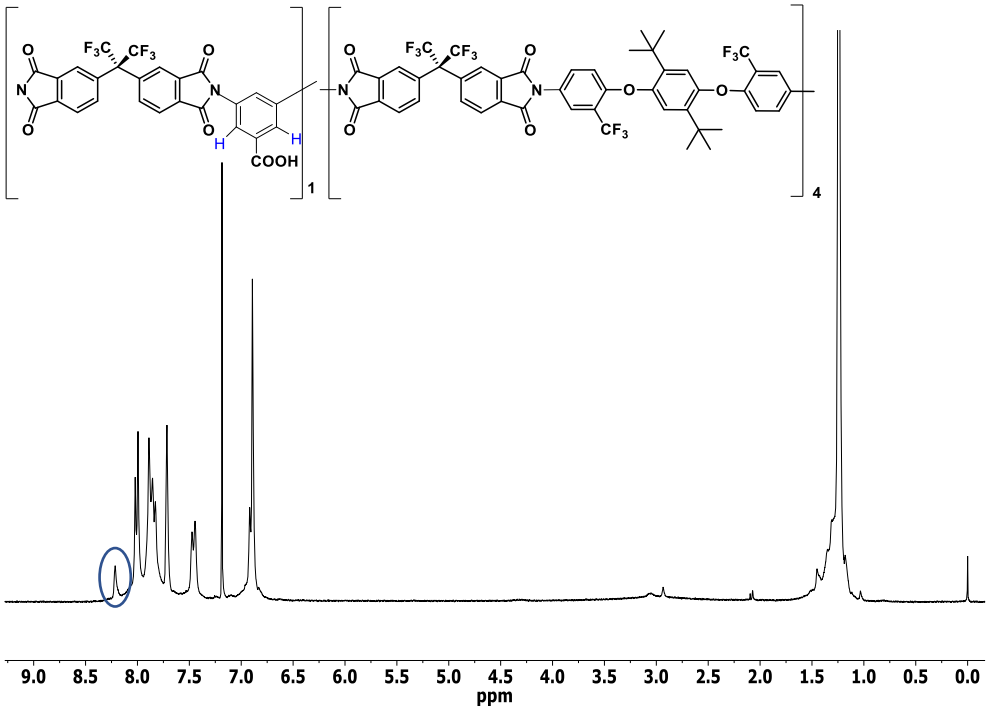

Figure 5. Spectra of ^{1}H-RMN of the COPOL-DABA(1/4). The NMR peak enclosed in the blue ellipse corresponds to the *ortho* hydrogens to the carboxylic groups of the DABA moiety

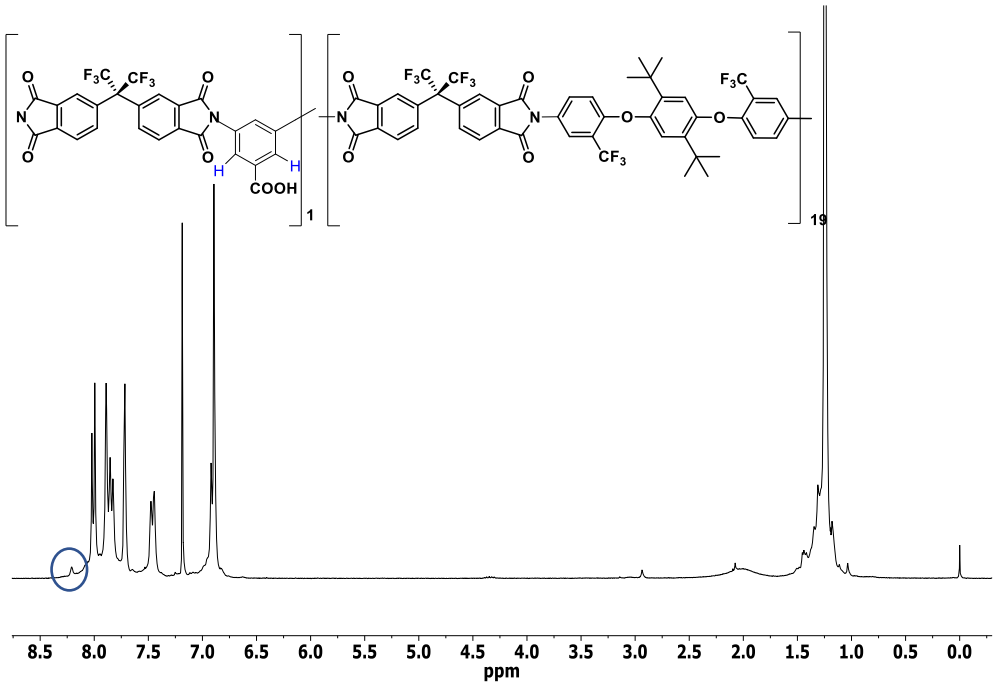

Figure 6. Spectra of ^{1}H-RMN of COPOL-DABA(1/19). The NMR peak enclosed in the blue ellipse corresponds to the *ortho* hydrogens to the carboxylic groups of the DABA moiety

3.2.2 ATR-FTIR spectroscopy

Figure 7 shows the ATR-FTIR spectra of the films of the copolymers and the corresponding crosslinks, as well as that of the homopolymer. As can be seen, the patterns of the copolymers showed no significant differences concerning that of the homopolyimide. It should be noted that the modification was small, and therefore, the 1/4 and 1/19 ratios of DABA to CF_3TBAPB make it difficult to appreciate the changes in their chemical structures.

Preprints (www.preprints.org) | NOT PEER-REVIEWED | Posted: 16 November 2022 doi:10.20944/preprints202211.0309.v1

Thus, the stress vibration of the -OH groups, which appears as a broad band between 3000-3600 cm^{-1} when the DABA content is high, could not be observed[74].

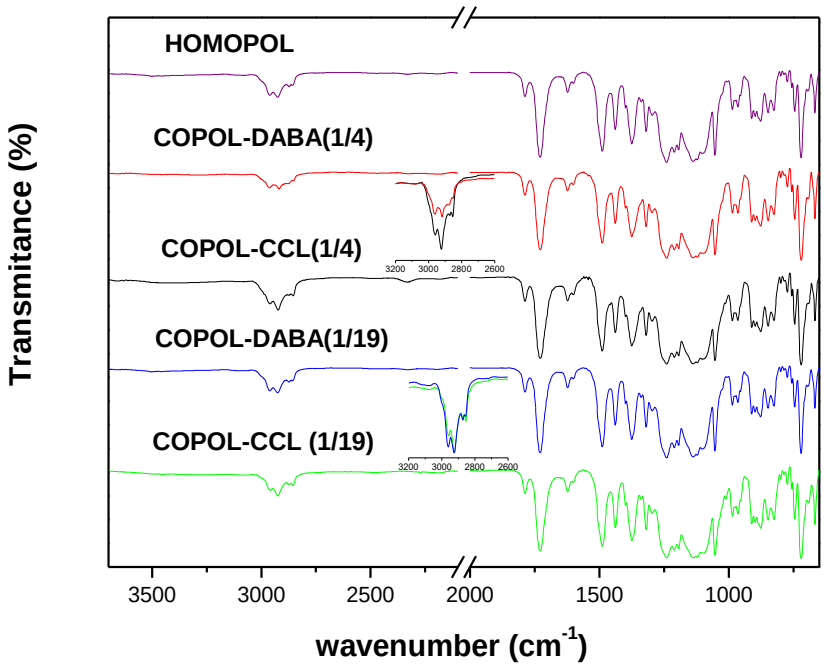

Figure 7. ATR-FTIR spectra for the homopolymer, the copolyimides, and the crosslinked homologs. The insets in the graphs show the broadened region around 2900 cm^{-1}.

When comparing the patterns of the copolyimides with those of their crosslinked counterparts, only small changes were observed in the region corresponding to the aliphatic C-H stress vibrations, around 2900 cm^{-1}. However, it should be taken into account that this zone showed the bands of the *tert*-butyl groups of the CF_3TBAPB diamine and those of the aliphatic chains of the crosslinking agent (1,4-butanediol), and they appeared to overlap. In conclusion, the ATR-FTIR technique was not suitable to characterize and evaluate the crosslinking of the copolymer membranes.

3.2.3 Elemental analysis

The elemental analyses of the copolyimides and the crosslinked films are shown in Table 2. Comparing the theoretical and experimental values, it can be seen that the values obtained for the copolyimides are close to the theoretical ones, although the differences observed in the case of the crosslinked copolyimides were somewhat larger.

Preprints (www.preprints.org) | NOT PEER-REVIEWED | Posted: 16 November 2022 doi:10.20944/preprints202211.0309.v1

Table 2. Elemental analysis of copolyimides and their crosslinked counterparts.

Polymer	%C Theoretical/found	%H Theoretical/found	%N Theoretical/found
COPOL-DABA(1/4)	58.8/ 58.7	3.1/ 3.3	3.4/ 3.1
COPOL-CCL-(1/4)	59.1*/58.5 58.9**	3.2*/3.0 3.2**	3.3*/3.0 3.3**
COPOL-DABA(1/19)	59.3/ 59.2	3.3 / 3.5	3.1/ 2.9
COPOL-CCL-(1/19)	59.4*/58.3 59.4**	3.3*/3.3 3.4**	3.0*/2.8 3.03**

* Theoretical % assuming 100% crosslinking. **Theoretical % assuming -OH-terminal modifications (monoester entities).

3.2.4 X-ray diffraction (WAXS)

Figure 8 compares the diffraction patterns of copolymers films, crosslinked films, and the homopolymer. All of them showed an amorphous nature. At first glance, the major difference between the copolymer profiles with that of the homopolymer consisted of the decrease in intensity, or even in some cases the disappearance of the peak at low angles. This maximum peak could be associated with an intramolecular distance of 18.4 Å ($\theta = 4.8$ °), which could be related to the preference of the chains to adopt extended conformations. However, it can be also commented that the arrangement of the chains depends on many parameters such as the imidization temperature, the heating rate, the type of substrate on which the film is prepared, and the thickness of the film, among others, which could justify the fact that sometimes a peak is detected or not.

Preprints (www.preprints.org) | NOT PEER-REVIEWED | Posted: 16 November 2022 doi:10.20944/preprints202211.0309.v1

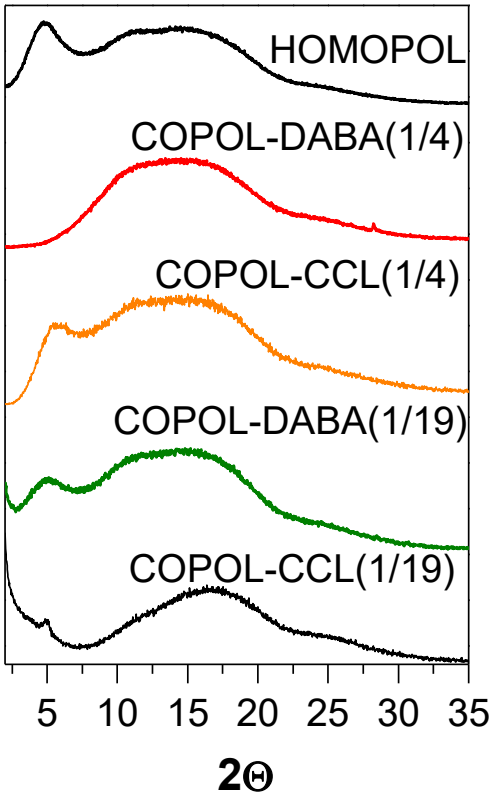

Figure 8. WAXS diffractograms of the homopolymer, DABA-derived copolyimides, and their corresponding crosslinked homologs.

Concerning crosslinked films, the COPOL-CCL(1/19) pattern seems to show a lower contribution to diffraction on the low-angle side of the amorphous halo. This fact could normally be associated with a higher packing of the chains. Chung et. al. [55] commented that the maximum of the amorphous halo, which corresponded to the most probable intersegmental distance or spacing, was greater the higher the degree of crosslinking. They stated that when only mono-esterification reactions occurred, i.e. one -OH group of the diol remains unreacted with no crosslinking, the d-spacing was smaller. Taking these considerations into account, it could be thought that the lower contribution of large d-spacings to the amorphous halo of COPOL-CCL(1/19) was due to a high degree of mono-esterification.

3.2.5 Solubility

Solubility is one of the fastest and most effective methods for testing crosslinking in polymeric materials. Crosslinking, by forming a network of infinite molecular weight, results in insolubility, although in membranes with small degrees of crosslinking, swelling or partial solubility of the membranes is also often observed. Table 3 shows the solubilities in different solvents of the membranes studied.

Preprints (www.preprints.org) | NOT PEER-REVIEWED | Posted: 16 November 2022 doi:10.20944/preprints202211.0309.v1

Table 3. Solubility of copolyimides.

Polymer	$CHCl_3$	THF	DMAc	NMP	m-Cresol
COPOL-DABA(1/4)	+ +	+ +	+ +	+ +	+ +
COPOL-CCL(1/4)	+ -	+ -	+ -	+ -	+-
COPOL-DABA(1/19)	+ +	+ +	+ +	+ +	+ +
COPOL-CCL(1/19)	+	+	+	+	+

Legend applied: + +cold soluble, +hot soluble, +- partially soluble in hot, - insoluble.

Copolyimide membranes exhibited excellent solubilities in common solvents. It was also observed that the COPOL- CCL(1/4) crosslinked membrane swelled when the solvent was heating, dissolving partially, while COPOL- CCL(1/19) dissolved completely in all solvents tested, which seems to indicate that this membrane was either not cross-linked or showed a very low degree of crosslinking.

3.2.6 Thermal properties

Figure 10 presents the calorimetry curves (DSC) of the copolyimides and their cross-linked homologs. Table 4 lists the glass transition temperature values, Tg, for the copolyimides and their crosslinked homologs.

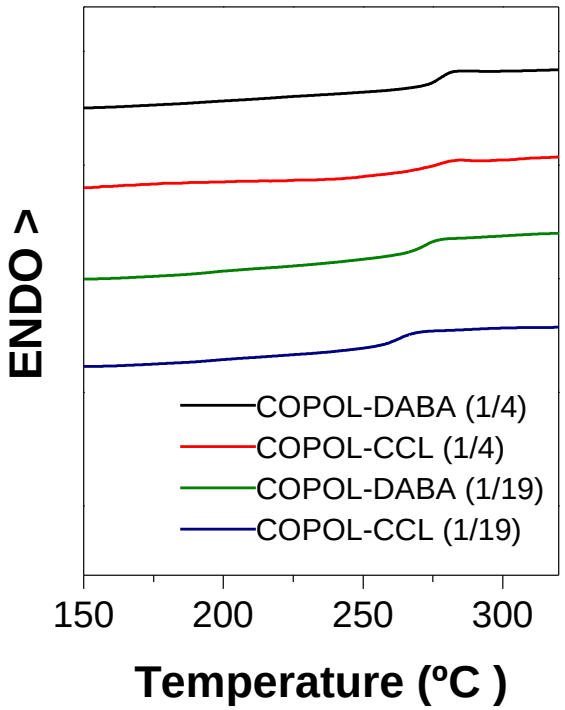

Figure 10. DSC of copolyimides and their corresponding crosslinked films.

In general, Tgs were higher than 260 °C. Moreover, the Tg of the copolyimides depended on the amount of carboxylic groups, the higher the content, the higher the Tg will be. On the other hand, COPOL-DABA(1/4) and its crosslinked counterpart showed the same Tg. However, COPOL-CCL(1/19) presented a Tg 10 °C lower than the non-crosslinked copolyimide, even though the -COOH content was lower, and therefore the degree of possible crosslinking should also be lower. This fact could be justified by the presence of unreacted crosslinking reagent, which was embedded inside the membrane and produced a plasticizing effect.

Preprints (www.preprints.org) | NOT PEER-REVIEWED | Posted: 16 November 2022 doi:10.20944/preprints202211.0309.v1

The comparison with the homopolymer 6FDA-CF_3TBAPB (Tg = 270 °C) showed an expected behavior. Thus, the copolyimide with the larger proportion of DABA monomer presented the higher Tg, due to, on the one hand, the rigidity conferred by this monomer and on the other hand, it could also be attributed to the presence of hydrogen bonds that occur between the carboxyl groups, while in the case of COPOL-DABA(1/19) no difference was appreciated, due to the small proportion of DABA present in the copolymer.

The most commonly accepted mechanism of degradation and/or weight loss associated with carboxylic groups is that described by Kratochvil et. al. [74,75], in which it is assumed that the -COOH groups first react with each other to form a dianhydride, which subsequently decarboxylates, at much higher temperatures, to form phenyl radicals that can crosslink the polymer chains.

The decarboxylation process usually occurs between 350-400 °C (depending on the Tg of the polymer), although it has been reported that this crosslinking can occur at temperatures 50 °C below [9]. On the other hand, it has been published that it is possible to produce crosslinking in polyimides with -CF_3 groups by treatment at elevated temperatures [76]. In this work, it was observed, by using a TGA coupled to a mass spectrometer (MS), that one of the first by-products in the decomposition of this type of polyimide was HCF_3. Thus, it is possible that at the same time as the acid groups are pyrolyzed, some CF_3 groups are also pyrolyzed with the result of a more crosslinked polyimide. Figure 11 shows the crosslinking mechanisms proposed in the literature and the possible crosslinking points [51,57,62].

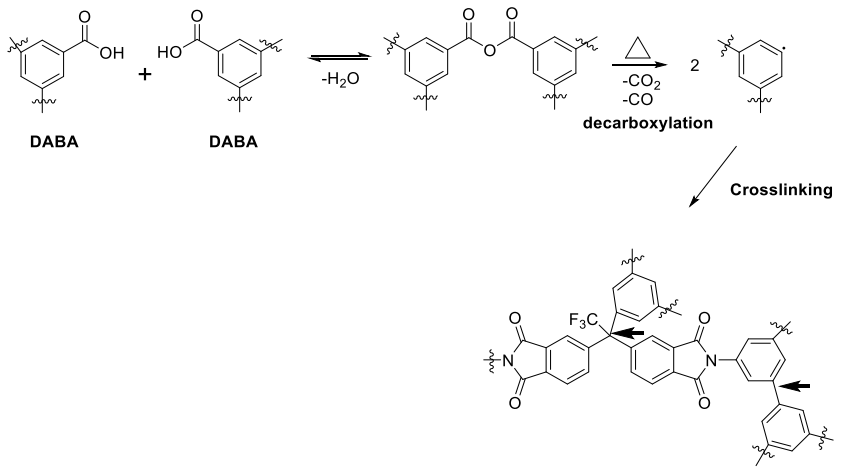

Figure 9. The proposed crosslinking mechanism for copolymers incorporating DABA monomer and CF_3 groups[75] (bold arrows represent the plausible crosslinking points).

Figure 11 shows the thermogravimetric curves, in a nitrogen atmosphere, of the copolymer films and those of the crosslinked copolymers. In addition, Table 4 shows the onset of degradation temperatures, Td, and carbonaceous residues (char yield, Rc) at 800 °C under N_2 (the Table also includes the values corresponding to the homopolymer 6FDA-CF_3TBAPB).

In our copolyimides, COPOL-DABA(1/4) showed a well-defined weight loss step (Td of 375 °C), corresponding to the loss of acid groups (approximately 2% loss), while COPOL-DABA(1/19) showed only a small continued loss (0.5% between 350 - 400 °C) until the onset of generalized chain degradation, which was similar for both copolyimides to the Td of the homopolymer.

Preprints (www.preprints.org) | NOT PEER-REVIEWED | Posted: 16 November 2022 doi:10.20944/preprints202211.0309.v1

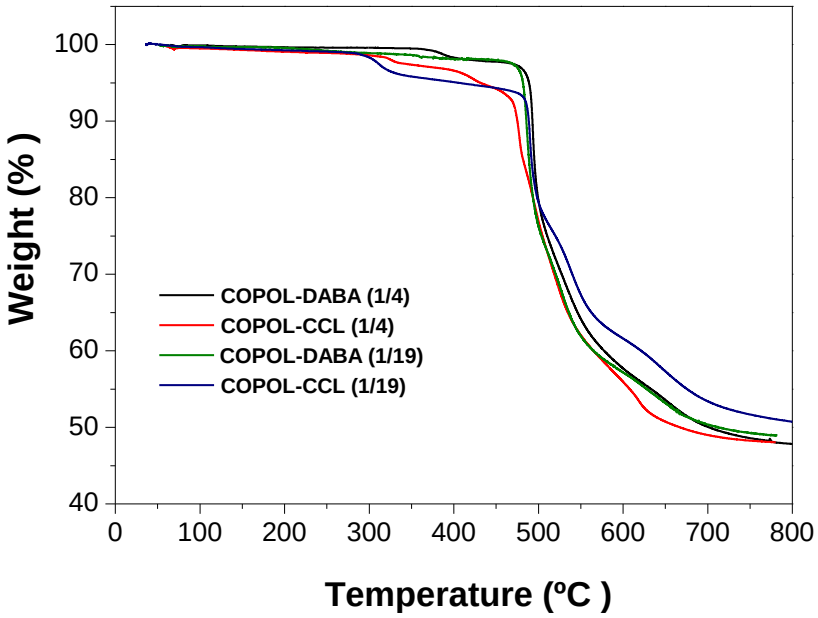

Figure 11. Thermograms of the copolyimides and their crosslinked counterparts.

Table 4. Glass transition temperatures, degradation temperatures, and char yield (% at 800 ºC), under nitrogen atmosphere, of homopolymer and copolyimides, and crosslinked polyimides. Inherent viscosity values of homopolyimide and copolyimides.

Polymer	Tg (ºC)	Td (°C)	Rc (%)	ηinh (dL.g-1
HOMOPOL	270	490	40	1.09
COPOL-DABA(1/4)	280	375/490	47	0.69
COPOL-CCL(1/4)	280	315/400/480	50	-
COPOL-DABA(1/19)	270	480	49	0.66
COPOL-CCL(1/19)	260	295/490	51	-

The crosslinked films also exhibited a small weight loss step before generalized chain degradation. In this case, the Tds were considerably lower than those observed for COPOL-DABA(1/4). In addition, COPOL-CCL(1/4) presented a small additional step at a temperature of 400 °C.

The weight losses in the first step can be associated with the loss of residual reagent, followed by the degradation of mono- or di-esterified chains. TGA showed that the COPOL-CCL(1/19) membrane had a higher amount of unreacted reagent. Furthermore, the solubility of this polymer indicated, as commented, that the degree of crosslinking was not high, so many acid groups would be mono-esterified, and consequently, this polymer would have lower thermal stability[50].

The crosslinking that occurs in these materials, either by the covalent crosslinking carried out or by the thermal crosslinking derived from the thermolysis of the -COOH groups, gave rise to higher carbon residues than those observed for the 6FDA-CF_3TBAPB homopolymer.

Preprints (www.preprints.org) | NOT PEER-REVIEWED | Posted: 16 November 2022 doi:10.20944/preprints202211.0309.v1

3.2.7 Inherent viscosity of homopolymer and copolyimides

The inherent viscosities of the copolyimides, determined to compare them with that of the homopolymer, and thus to get an approximate idea about the molecular weight obtained, are shown in Table 4. GPC measurements were not carried out, since there was a risk that the polymers would be retained in the column due to the presence of acid groups.

The viscosities were not as high as that of the homopolymer. However, the good values observed in the mechanical properties (as will be detailed later), indicated that these molecular weights were sufficiently high to allow for a study of these polymeric films as gas separation membranes at high pressures.

3.2.8 Density and fractional free volume (FFV)

In none of the publications on polyimide crosslinking, nor those dealing with DABA derivatives, FFV data were found. In the case of crosslinked membranes, the determination of FFV is quite cumbersome since the final structure of the polymer is not known, and therefore the determination of the molecular volume has a significant error. That is unless quantitative reactions are assumed, the determination of V_W volumes is not possible, and only the use of techniques that directly determine the FFV value, for example, using the PALS technique, would produce an accurate and rigorous analysis of the FFV (and its distribution) [77].

However, it was possible to determine the FFV values of the copolyimides (Table 5).

Table 5. Film densities of homopolyimide, copolyimides, and crosslinked polyimides. Fractional free volumes (FFV) of homopolyimide, and copolyimides

Polymer	ρ (g.cm-3)	FFV
HOMOPOL	1.291	0.238
COPOL-DABA(1/4)	1.301	0.235
COPOL-CCL(1/4)	1.340	-
COPOL-DABA(1/19)	1.295	0.233
COPOL-CCL(1/19)	1.334	-

The trend in the density values obtained agreed with those described in the literature[78]. Thus, the copolyimides presented FFV values comparable (within the experimental error) to the homopolyimide. On the other hand, the crosslinked films presented higher densities than their counterparts without crosslinking (3% higher), although no significant conclusion could be drawn due to the solvent, and crosslinking reagent, embedded in the samples.

3.2.9 Mechanical properties

Table 6 shows the Young's modulus, tensile strength, and elongation at break values of the copolyimide films, the crosslinked copolyimide films, and the homopolymer. The polymer films exhibited similar Young's moduli, higher than 1.8 GPa. The crosslinked films showed higher Young moduli and lower tensile strength values than the copolyimides and the homopolymer. In addition, crosslinked films also showed lower elongation at break values, approximately half that of the non-crosslinked films.

Preprints (www.preprints.org) | NOT PEER-REVIEWED | Posted: 16 November 2022 doi:10.20944/preprints202211.0309.v1

Table 6. Mechanical properties of polymers

Polymer	Young Modulus (GPa)	Tensile strength (MPa)	Elongation at break (%)
HOMOPOL	1.6±0.1	91±10	9±2
COPOL-DABA(1/4)	1.7±0.2	96±18	9±1
COPOL-CCL-(1/4)	1.9±0.1	75±12	5±1
COPOLDABA(1/19)	1.9±0.1	105±5	10±2
COPOL-CCL-(1/19)	2.1±0.1	88±4	5.7±0.2

3.3 Gas separation properties: permeability, selectivity, and plasticization study

3.3.1 Permeability and selectivity of membranes

Table 7 shows the gas separation results obtained for the homopolyimide, DABA-derived copolyimides, and covalently crosslinked polymers. These data were compared with the results presented previously for the 6FDA- CF_3TBAPB(C) homopolymer.

Table 7. Permeability (P)a and ideal selectivity (α) coefficients for linear and crosslinked copolyimides (measurement conditions: 3 bar at 30 °C)

Polymer	He	N_2	O_2	CH_4	CO_2	$\alpha O_2/N_2$	$\alpha CO_2/CH_4$
HOMOPOL	230	8.7	38	6.4	150	4.3	23
COPOL-DABA(1/4)	200	6.1	30	4.5	120	4.9	27
COPOL-CCL(1/4)	180	5.4	26	3.8	110	4.9	29
COPOLDABA(1/19)	170	5.1	25	3.7	100	4.8	28
COPOL-CCL(1/19)	140	3.8	19	2.7	75	4.9	28

Permeability in Barrer. 1 Barrer = 10^{-10} cm^3 (STP) cm/cm^2 s cmHg.

A decrease in permeability to all gases when comparing these copolyimides with the homopolymer was observed. Thus, the substitution, even in very small proportions, of the diamine CF_3TBAPB by the diamine DABA, resulted in a decrease in permeability for both copolyimides. The selectivity underwent an important improvement that could be associated with a greater intrinsic rigidity of the chains, introduced by the DABA diamine, and for the existence of polar groups that can interact with certain gases. However, it could be seen that there seems to be an inverse relationship between the amount of COOH groups present in the polymeric matrix and their effect on permeability (both for the O_2/N_2 gas pair and for the CO_2/CH_4 one).

Thus, it was observed that the membrane with a lower amount of DABA in its structure presented a more pronounced decrease in permeability:

$$P_{HOMOPOL} > P_{COPOL\text{-}DABA(1/4)}) > P_{COPOL\text{-}DABA(1/19)}.$$

With the introduction of 20% DABA in the main chain, COPOL- DABA(1/4), the permeability for both O_2 and CO_2 was reduced by 20% relative to the homopolymer. However, with the introduction of only 5% DABA in the main chain, COPOL-DABA(1/19), the permeability was reduced by more than 30% for CO_2 and 50% for O_2. This behavior is strange and we could not find an explanation for this anomalous fact.

Preprints (www.preprints.org) | NOT PEER-REVIEWED | Posted: 16 November 2022 doi:10.20944/preprints202211.0309.v1

In the case of the crosslinked membranes, a decrease in permeability values was observed when compared with the non-crosslinked counterparts, which did not translate into an improvement in selectivity. The material with the lowest content of carboxyl groups had the lowest permeabilities, which could be due to the higher amount of residual reagent present inside the membrane. No differences in O_2/N_2 and CO_2/CH_4 selectivities were observed between the crosslinked membranes and the reference copolyimides.

the degree of productivity of the membranes was determined, by plotting these systems in graphs of permeability vs selectivity where Robeson limits[79,80] were included. Figures 11 and 12 plot Selectivity (α O_2/N_2 and α CO_2/CH_4) vs Permeability to the most permeable gas of both mixtures (PO_2 and PCO_2, respectively).

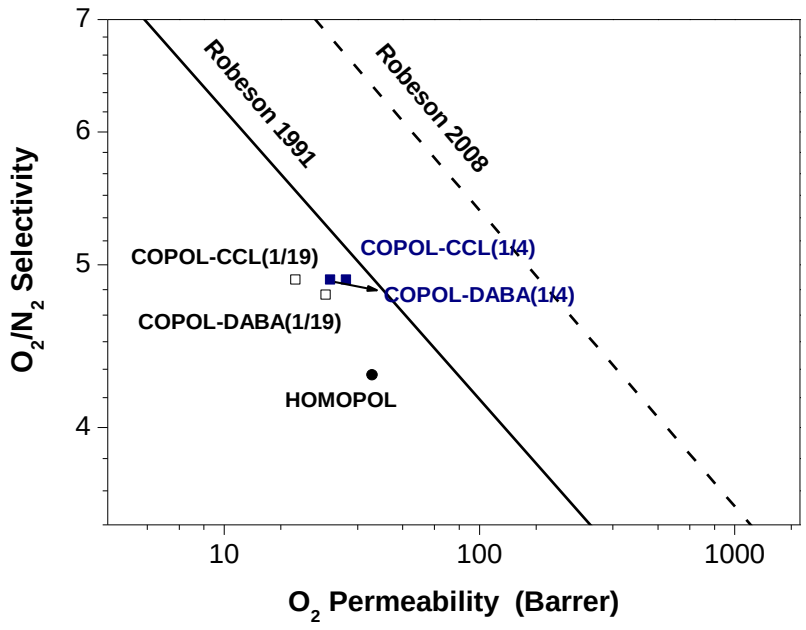

Figure 12. Selectivity O_2/N_2 *vs* Permeability O_2.

Figure 12 shows the improvements in selectivity, for the copolyimides and crosslinked copolyimides compared to the homopolymer for the O_2/N_2 gas pair. The permeabilities of all of them were comparable, except for COPOL-CCL(1/19) which was lower.

Therefore, the objective of improving the gas separation properties of the homopolymer (polyimide 6FDA-CF_3TBAPB) in this series of copolyimides has been achieved. It could be concluded that the introduction of -COOH groups in the polymeric structure in the ratio used (1/4) and (1/19) lead to an enhancement in the permeability/selectivity balance for air purification processes since the loss in permeability was not very pronounced in comparison with the selectivity improvement.

Preprints (www.preprints.org) | NOT PEER-REVIEWED | Posted: 16 November 2022 doi:10.20944/preprints202211.0309.v1

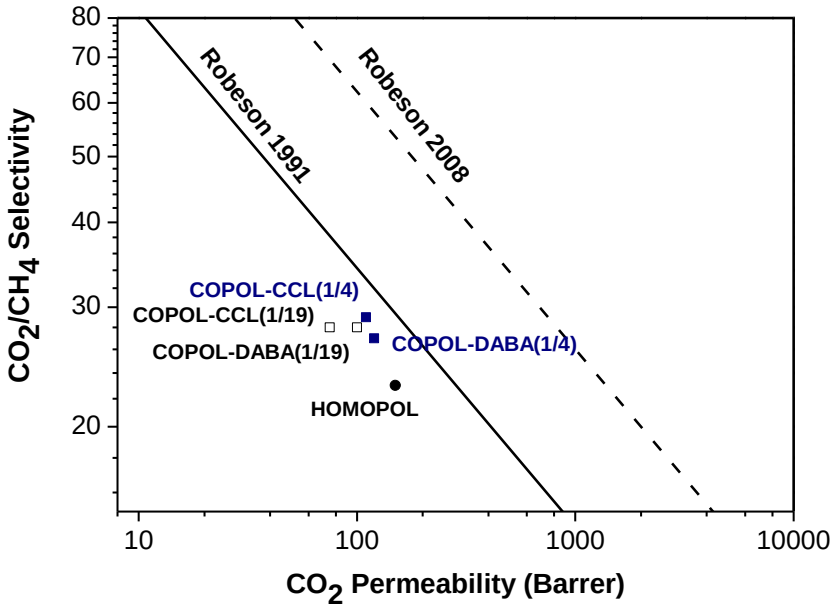

Figure 13. Selectivity CO_2/CH_4 *vs* CO_2 Permeability.

In the case of the CO_2/CH_4 gas pair (Figure 13), a similar behavior was observed. In other words, an increase in selectivity was observed in all cases having a slight loss of permeability.

In conclusion, the excellent results obtained in the gas separation measurements confirmed that the COPOL-DABA(1/4), COPOL-DABA(1/19), and COPOL-CCL(1/4) membranes showed good permeation properties and they were more selective than the 6FDA-CF_3TBAPB homopolymer. Therefore, it can be stated that using a simple, cheap, and easy-to-perform copolymerization with the DABA monomer, it was possible to improve the separation properties for several gas mixtures. However, it should be noted that in the case of COPOL-DABA(1/19), having a very low DABA content, it was not possible to obtain the desired degree of crosslinking. This fact must be added to the impossibility of not having been able to eliminate the excess of the crosslinking reagent with the heat treatment applied.

3.3.2 Plasticization Study

Finally, a study was carried out to determine the tendency of these membranes to undergo plasticization processes. This study consisted of monitoring the changes in permeability in each of the membranes when CO_2 passed through them at different pressures. The plasticization pressure, Pp, or pressure at which the increase in permeability begins to occur if it exists, could be obtained[22,81].

Figure 14 shows the CO_2 permeability data at different measurement pressures. The CO_2 pressures used were: 3, 5, 7, 9, 11, 13, 15, 20, 25, and 30 bar.

Preprints (www.preprints.org) | NOT PEER-REVIEWED | Posted: 16 November 2022 doi:10.20944/preprints202211.0309.v1

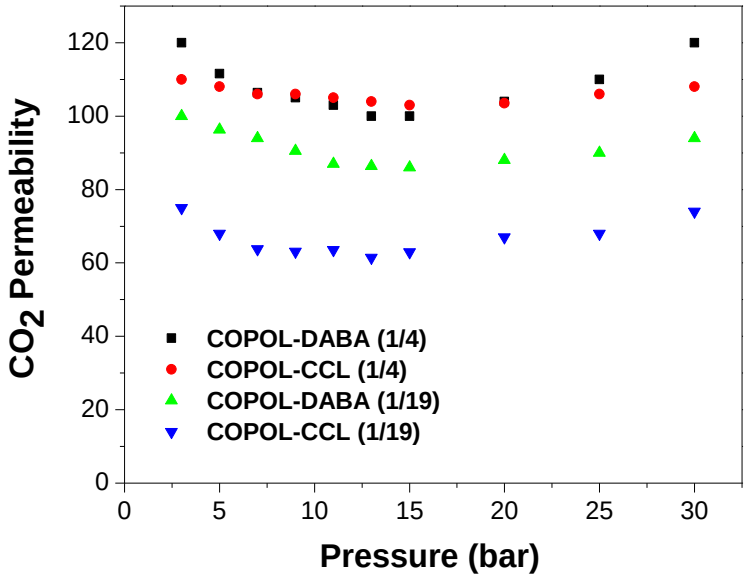

Figure 14. CO_2 Permeability *vs* Pressure.

The behavior shown by the membranes agreed with that described in the literature for copolyimides derived from 6FDA and DABA. In the copolyimide membranes with free -COOH groups, COPOL-DABA(1/4) and COPOL-DABA(1/19), plasticization pressures were observed in the zone between 15 and 20 bar. However, the increase in permeability, that occurs from this pressure, was much less pronounced than that observed for most of the polyimides reported in the literature, where permeability generally increases more sharply above that pressure value. Thus, it can be said that the copolyimides derived from CF_3TBAPB, and having DABA as comonomer, presented an improved plasticization resistance when compared with other polyimides derived from the 6FDA dianhydride.

For the COPOL-CCL(1/4) crosslinked membrane, it was observed, when compared with the precursor copolyimide, a considerable decrease in the curvature of the graph, so, the increase in permeability from the plasticization pressure point was much lower.

In the case of COPOL-CCL(1/19), a slightly lower plasticization pressure was observed than that of the starting membrane COPOL-DABA(1/19), which seems to confirm that this membrane is not crosslinked and contains a large amount of crosslinking reagent. This statement is in agreement with the previously cited work of Hess et al [63].

In this work, important differences have been observed between the copolyimide membrane having free acid groups, its cross-linked counterpart, and the non-crosslinked one, which is a membrane with mostly mono-esterification moieties. As can be seen in Figure 13, it was observed that the COPOL-DABA cross-linked membrane (1/4) presented a low tendency to plasticize together with good permeability properties. This result allows us to consider that the approach of incorporating small percentages of DABA, as a comonomer able to undergo crossling reactions, in homopolymers having high free volume fractions and permeability, is a valid approach to obtaining materials with excellent gas separation properties.

4. Conclusions

As the main conclusion, we can say that the design, and synthesis, of these copolymers and covalently crosslinked copolymers have been successful since membranes with good gas separation productivities have been obtained even working at high CO2 pressures.

However, it is clear that to know the real applicability of these materials in gas separation at the industrial level, it would be necessary to study them more exhaustively.

In particular, it seems necessary to know their resistance to plasticization in long-term separation processes and, above all, to study their behavior in real gas mixtures at high gas pressures and gas temperatures.

Author Contributions: Conceptualization, Cristina Álvarez, and Ángel E. Lozano; Formal analysis, Noelia Esteban, Marta Juan-y-Seva, Carla Aguilar-Lugo, Jesús A. Miguel and Claudia Staudt; Funding acquisition, Jesús A. Miguel, Jose G. Campa, and Ángel E. Lozano; Investigation, Noelia Esteban and Marta Juan-y-Seva; Methodology, Cristina Álvarez, and Ángel E. Lozano; Project administration, Ángel E. Lozano; Resources, Jesús A. Miguel, Jose G. Campa, Cristina Álvarez and Ángel E. Lozano; Supervision, Claudia Staudt and Ángel E. Lozano; Validation, Marta Juan-y-Seva, Carla Aguilar-Lugo, Claudia Staudt and Jose G. Campa; Writing – original draft, Noelia Esteban, Marta Juan-y-Seva, Carla Aguilar-Lugo, Cristina Álvarez, and Ángel E. Lozano; Writing – review & editing, Noelia Esteban, Marta Juan-y-Seva, Jesús A. Miguel, Jose G. Campa, Cristina Álvarez and Ángel E. Lozano. All authors have read and agreed to the published version of the manuscript.

Funding: This research was funded by Spain's Agencia Estatal de Investigación (AEI) (Projects: PID2019-109403RB-C22 (AEI/FEDER, UE), PID2019-109403RB-C21 (AEI/FEDER, UE) and PID2020-118547GB-I00 (AEI/FEDER, UE)) and by the Spanish Junta de Castilla y León (VA224P20).

Institutional Review Board Statement: Not applicable.

Data Availability Statement: Not applicable.

Acknowledgments: In this section, you can acknowledge any support given which is not covered by the author contribution or funding sections. This may include administrative and technical support, or donations in kind (e.g., materials used for experiments).

Conflicts of Interest: The authors declare no conflict of interest.

References

1. Ma, X.-H.; Yang, S.-Y. Polyimide Gas Separation Membranes. In *Advanced Polyimide Materials*; Elsevier, 2018; pp. 257–322 ISBN 9780128126400.
2. Liang, C. Z.; Chung, T.-S. S.; Lai, J.-Y. Y. A review of polymeric composite membranes for gas separation and energy production. *Prog. Polym. Sci.* **2019**, *97*, 101141, doi:10.1016/j.progpolymsci.2019.06.001.
3. Liu, Y.; Liu, Z.; Liu, G.; Qiu, W.; Bhuwania, N.; Chinn, D.; Koros, W. J. Surprising plasticization benefits in natural gas upgrading using polyimide membranes. *J. Memb. Sci.* **2020**, *593*, 117430, doi:10.1016/j.memsci.2019.117430.
4. Chang, Y. S.; Kumari, P.; Munro, C. J.; Szekely, G.; Vega, L. F.; Nunes, S.; Dumée, L. F. Plasticization mitigation strategies for gas and liquid filtration membranes - A review. *J. Memb. Sci.* **2023**, *666*, 121125, doi:10.1016/j.memsci.2022.121125.
5. Wessling, M.; Schoeman, S.; van der Boomgaard, T.; Smolders, C. A. Plasticization of gas separation membranes. *Gas Sep. Purif.* **1991**, *5*, 222–228, doi:10.1016/0950-4214(91)80028-4.
6. Baker, R. W.; Lokhandwala, K. Natural gas processing with membranes: An overview. *Ind. Eng. Chem. Res.* **2008**, *47*, 2109–2121, doi:10.1021/ie071083w.
7. Vu, D. Q.; Koros, W. J.; Miller, S. J. Effect of condensable impurities in CO2/CH4 gas feeds on carbon molecular sieve hollow-fiber membranes. *Ind. Eng. Chem. Res.* **2003**, *42*, doi:10.1021/ie020698k.
8. Sanaeepur, H.; Ebadi Amooghin, A.; Bandehali, S.; Moghadassi, A.; Matsuura, T.; Van der Bruggen, B. Polyimides in membrane gas separation: Monomer's molecular design and structural engineering. *Prog. Polym. Sci.* **2019**, *91*, 80–125, doi:10.1016/j.progpolymsci.2019.02.001.

9. Qiu, W.; Chen, C.-C.; Xu, L.; Cui, L.; Paul, D. R.; Koros, W. J. Sub- T g Cross-Linking of a Polyimide Membrane for Enhanced CO 2 Plasticization Resistance for Natural Gas Separation. *Macromolecules* **2011**, *44*, 6046–6056, doi:10.1021/ma201033j.
10. Wind, J. D.; Paul, D. R.; Koros, W. J. Natural gas permeation in polyimide membranes. *J. Memb. Sci.* **2004**, *228*, 227–236, doi:10.1016/j.memsci.2003.10.011.
11. Favvas, E. P.; Katsaros, F. K.; Papageorgiou, S. K.; Sapalidis, A. A.; Mitropoulos, A. C. A review of the latest development of polyimide based membranes for CO2 separations. *React. Funct. Polym.* **2017**, *120*, 104–130, doi:10.1016/j.reactfunctpolym.2017.09.002.
12. Zhang, M.; Deng, L.; Xiang, D.; Cao, B.; Hosseini, S.; Li, P. Approaches to Suppress CO2-Induced Plasticization of Polyimide Membranes in Gas Separation Applications. *Processes* **2019**, *7*, 51, doi:10.3390/pr7010051.
13. Nemestóthy, N.; Bakonyi, P.; Lajtai-Szabó, P.; Bélafi-Bakó, K. The impact of various natural gas contaminant exposures on co2/ch4 separation by a polyimide membrane. *Membranes (Basel).* **2020**, *10*, 1–10, doi:10.3390/membranes10110324.
14. Han, W.; Zhang, C.; Weng, Y. Preparation and research progress of polyimide membranes in gas separation with anti-plasticization property. *Sci. Sin. Chim.* **2020**, *50*, doi:10.1360/SSC-2020-0021.
15. Ren, Y.; Liang, X.; Dou, H.; Ye, C.; Guo, Z.; Wang, J.; Pan, Y.; Wu, H.; Guiver, M. D.; Jiang, Z. Membrane-Based Olefin/Paraffin Separations. *Adv. Sci.* **2020**, *7*, 1–29, doi:10.1002/advs.202001398.
16. Tanaka, K.; Taguchi, A.; Hao, J.; Kita, H.; Okamoto, K. Permeation and separation properties of polyimide membranes to olefins and paraffins. *J. Memb. Sci.* **1996**, *121*, 197–207, doi:10.1016/S0376-7388(96)00182-2.
17. Faiz, R.; Li, K. Polymeric membranes for light olefin/paraffin separation. *Desalination* **2012**, *287*, 82–97, doi:10.1016/j.desal.2011.11.019.
18. Velioğlu, S.; Ahunbay, M. G.; Tantekin-Ersolmaz, S. B. Propylene/propane plasticization in polyimide membranes. *J. Memb. Sci.* **2016**, *501*, 179–190, doi:10.1016/j.memsci.2015.11.034.
19. Okamoto, K. Permeation and separation properties of polyimide membranes to 1,3-butadiene and n-butane. *J. Memb. Sci.* **1997**, *134*, 171–179, doi:10.1016/S0376-7388(97)00128-2.
20. Tiwari, R. R.; Jin, J.; Freeman, B. D.; Paul, D. R. Physical aging, CO 2 sorption and plasticization in thin films of polymer with intrinsic microporosity (PIM-1). *J. Memb. Sci.* **2017**, *537*, 362–371, doi:10.1016/j.memsci.2017.04.069.
21. Wessling, M.; Huisman, I.; Boomgaard, T. v.d.; Smolders, C. A. Time-dependent permeation of carbon dioxide through a polyimide membrane above the plasticization pressure. *J. Appl. Polym. Sci.* **1995**, *58*, doi:10.1002/app.1995.070581105.
22. Bos, A.; Pünt, I. G. M.; Wessling, M.; Strathmann, H. CO2-induced plasticization phenomena in glassy polymers. *J. Memb. Sci.* **1999**, *155*, 67–78, doi:10.1016/S0376-7388(98)00299-3.
23. Zhang, L.; Xiao, Y.; Chung, T. S.; Jiang, J. Mechanistic understanding of CO2-induced plasticization of a polyimide membrane: A combination of experiment and simulation study. *Polymer (Guildf).* **2010**, *51*, 4439–4447, doi:10.1016/j.polymer.2010.07.032.
24. Scholes, C. A.; Kentish, S. E.; Stevens, G. W. The effect of condensable minor components on the gas separation performance of polymeric membranes for carbon dioxide capture. *Energy Procedia* **2009**, *1*, 311–317, doi:10.1016/j.egypro.2009.01.043.
25. Bos, A.; Punt, I. G. M.; Wessling, M.; Strathmann, H. Suppression of CO2-plasticization by semiinterpenetrating polymer network formation. *J. Polym. Sci. Part B Polym. Phys.* **1998**, *36*, 1547–1556, doi:10.1002/(SICI)1099-0488(19980715)36:9<1547::AID-POLB12>3.0.CO;2-5.
26. Duthie, X.; Kentish, S.; Powell, C.; Nagai, K.; Qiao, G.; Stevens, G. Operating temperature effects on the plasticization of polyimide gas separation membranes. *J. Memb. Sci.* **2007**, *294*, 40–49, doi:10.1016/j.memsci.2007.02.004.
27. Swaidan, R. J. Tuning PIM-PI-Based Membranes for Highly Selective Transport of Propylene/Propane, 2016.
28. Zhou, C. The accelerated CO2 plasticization of ultra-thin polyimide films and the effect of surface chemical cross-linking on plasticization and physical aging. *J. Memb. Sci.* **2003**, *225*, 125–134, doi:10.1016/j.memsci.2003.07.006.
29. Xia, J.; Chung, T. S.; Li, P.; Horn, N. R.; Paul, D. R. Aging and carbon dioxide plasticization of thin polyetherimide films. *Polymer (Guildf).* **2012**, *53*, doi:10.1016/j.polymer.2012.03.009.
30. Staudt-Bickel, C.; J. Koros, W. Improvement of CO2/CH4 separation characteristics of polyimides by chemical crosslinking.

J. Memb. Sci. **1999**, *155*, 145–154, doi:10.1016/S0376-7388(98)00306-8.

31. Houben, M.; Kloos, J.; van Essen, M.; Nijmeijer, K.; Borneman, Z. Systematic investigation of methods to suppress membrane plasticization during CO2 permeation at supercritical conditions. *J. Memb. Sci.* **2022**, *647*, 120292, doi:10.1016/j.memsci.2022.120292.
32. Balçık, M.; Velioğlu, S.; Tantekin-Ersolmaz, S. B.; Ahunbay, M. G. Can crosslinking improve both CO2 permeability and plasticization resistance in 6FDA–pBAPS/DABA copolyimides? *Polymer (Guildf).* **2020**, *205*, doi:10.1016/j.polymer.2020.122789.
33. Xu, R.; Li, L.; Jin, X.; Hou, M.; He, L.; Lu, Y.; Song, C.; Wang, T. Thermal crosslinking of a novel membrane derived from phenolphthalein-based cardo poly(arylene ether ketone) to enhance CO2/CH4 separation performance and plasticization resistance. *J. Memb. Sci.* **2019**, doi:10.1016/J.MEMSCI.2019.05.084.
34. Deng, L.; Xue, Y.; Yan, J.; Lau, C. H.; Cao, B.; Li, P. Oxidative crosslinking of copolyimides at sub-Tg temperatures to enhance resistance against CO2-induced plasticization. *J. Memb. Sci.* **2019**, *583*, 40–48, doi:10.1016/j.memsci.2019.04.002.
35. Narzary, B. B.; Baker, B. C.; Yadav, N.; D'Elia, V.; Faul, C. F. J. Crosslinked porous polyimides: Structure, properties and applications. *Polym. Chem.* 2021, *12*.
36. Kammakakam, I.; Wook Yoon, H.; Nam, S. Y.; Bum Park, H.; Kim, T. H. Novel piperazinium-mediated crosslinked polyimide membranes for high performance CO2 separation. *J. Memb. Sci.* **2015**, *487*, doi:10.1016/j.memsci.2015.03.053.
37. Koros, W. J.; Mahajan, R. Pushing the limits on possibilities for large scale gas separation: Which strategies? *J. Memb. Sci.* **2001**, *181*, 141.
38. Katarzynski, D.; Pithan, F.; Staudt, C. Pervaporation of multi component aromatic/aliphatic mixtures through copolyimide membranes. *Sep. Sci. Technol.* **2008**, *43*, doi:10.1080/01496390701747911.
39. Pithan, F.; Staudt-Bickel, C. Crosslinked Copolyimide Membranes for Phenol Recovery from Process Water by Pervaporation. *Chemphyschem* **2003**, *4*, 967–973, doi:10.1002/cphc.200300707.
40. Wind, J. D.; Sirard, S. M.; Paul, D. R.; Green, P. F.; Johnston, K. P.; Koros, W. J. Carbon Dioxide-Induced Plasticization of Polyimide Membranes: Pseudo-Equilibrium Relationships of Diffusion, Sorption, and Swelling. *Macromolecules* **2003**, *36*, 6433–6441, doi:10.1021/ma0343582.
41. Wang, H.; Zhang, K.; Ho Li, J. P.; Huang, J.; Yuan, B.; Zhang, C.; Yu, Y.; Yang, Y.; Lee, Y.; Li, T. Engineering plasticization resistant gas separation membranes using metal–organic nanocapsules. *Chem. Sci.* **2020**, *11*, 4687–4694, doi:10.1039/D0SC01498B.
42. Isfahani, A. P.; Ghalei, B.; Wakimoto, K.; Bagheri, R.; Sivaniah, E.; Sadeghi, M. Plasticization resistant crosslinked polyurethane gas separation membranes. *J. Mater. Chem. A* **2016**, *4*, 17431–17439, doi:10.1039/C6TA07820F.
43. Wang, Y. C.; Huang, S. H.; Hu, C. C.; Li, C. L.; Lee, K. R.; Liaw, D. J.; Lai, J. Y. Sorption and transport properties of gases in aromatic polyimide membranes. *J. Memb. Sci.* **2005**, *248*, 15–25, doi:10.1016/j.memsci.2004.09.015.
44. Yu, H. J.; Chan, C.-H.; Nam, S. Y.; Yoo, J. S.; Lee, J. S. Thermally cross-linked ultra-robust membranes for plasticization resistance and permeation enhancement – A combined theoretical and experimental study. *J. Memb. Sci.* **2022**, 120250, doi:10.1016/j.memsci.2021.120250.
45. Thür, R.; Lemmens, V.; Van Havere, D.; van Essen, M.; Nijmeijer, K.; Vankelecom, I. F. J. Tuning 6FDA-DABA membrane performance for CO2 removal by physical densification and decarboxylation cross-linking during simple thermal treatment. *J. Memb. Sci.* **2020**, *610*, 118195, doi:10.1016/j.memsci.2020.118195.
46. Escorial, L.; de la Viuda, M.; Rodríguez, S.; Tena, A.; Marcos, A.; Palacio, L.; Prádanos, P.; Lozano, A. E.; Hernández, A. Partially pyrolized gas-separation membranes made from blends of copolyetherimides and polyimides. *Eur. Polym. J.* **2018**, *103*, 390–399, doi:10.1016/j.eurpolymj.2018.04.031.
47. Matesanz-Niño, L.; Aguilar-Lugo, C.; Prádanos, P.; Hernandez, A.; Bartolomé, C.; José, G.; Palacio, L.; González-Ortega, A.; Galizia, M.; Álvarez, C.; others; de la Campa, J. G.; Palacio, L.; González-Ortega, A.; Galizia, M.; Álvarez, C.; Lozano, Á. E. Gas separation membranes obtained by partial pyrolysis of polyimides exhibiting polyethylene oxide moieties. *Polymer*

(Guildf). **2022**, *247*, 124789, doi:10.1016/j.polymer.2022.124789.

48. Comesaña-Gándara, B.; de la Campa, J. G.; Hernández, A.; Jo, H. J.; Lee, Y. M.; de Abajo, J.; Lozano, A. E. Gas separation membranes made through thermal rearrangement of ortho-methoxypolyimides. *RSC Adv.* **2015**, *5*, 102261–102276, doi:10.1039/C5RA19207B.
49. Soto, C.; Comesaña-Gandara, B.; Marcos, Á.; Cuadrado, P.; Palacio, L.; Lozano, Á. E.; Álvarez, C.; Prádanos, P.; Hernandez, A. Thermally Rearranged Mixed Matrix Membranes from Copoly(o-hydroxyamide)s and Copoly(o-hydroxyamide-amide)s with a Porous Polymer Network as a Filler—A Comparison of Their Gas Separation Performances. *Membranes (Basel).* **2022**, *12*, 998, doi:10.3390/membranes12100998.
50. Huertas, R. M.; Doherty, C. M.; Hill, A. J.; Lozano, A. E.; de Abajo, J.; de la Campa, J. G.; Maya, E. M. Preparation and gas separation properties of partially pyrolyzed membranes (PPMs) derived from copolyimides containing polyethylene oxide side chains. *J. Memb. Sci.* **2012**, *409–410*, 200–211, doi:10.1016/j.memsci.2012.03.057.
51. Maya, E. M.; Tena, A.; de Abajo, J.; de la Campa, J. G.; Lozano, A. E. Partially pyrolyzed membranes (PPMs) derived from copolyimides having carboxylic acid groups. Preparation and gas transport properties. *J. Memb. Sci.* **2010**, *349*, 385–392, doi:10.1016/j.memsci.2009.12.001.
52. Puertas-Bartolomé, M.; Dose, M. E.; Bosch, P.; Freeman, B. D.; McGrath, J. E.; Riffle, J. S.; Lozano, A. E.; de la Campa, J. G.; Álvarez, C. Aromatic poly(ether ether ketone)s capable of crosslinking via UV irradiation to improve gas separation performance. *RSC Adv.* **2017**, *7*, 55371–55381, doi:10.1039/C7RA11018A.
53. Kita, H.; Inada, T.; Tanaka, K.; Okamoto, K. ichi Effect of photocrosslinking on permeability and permselectivity of gases through benzophenone- containing polyimide. *J. Memb. Sci.* **1994**, *87*, doi:10.1016/0376-7388(93)E0098-X.
54. Wind, J. D.; Staudt-Bickel, C.; Paul, D. R.; Koros, W. J. The effects of crosslinking chemistry on CO2 plasticization of polyimide gas separation membranes. *Ind. Eng. Chem. Res.* **2002**, *41*, doi:10.1021/ie0204639.
55. Shao, L.; Chung, T. S.; Goh, S. H.; Pramoda, K. P. Polyimide modification by a linear aliphatic diamine to enhance transport performance and plasticization resistance. *J. Memb. Sci.* **2005**, *256*, 46–56, doi:10.1016/j.memsci.2005.02.030.
56. Shao, L.; Chung, T. S.; Goh, S. H.; Pramoda, K. P. The effects of 1,3-cyclohexanebis(methylamine) modification on gas transport and plasticization resistance of polyimide membranes. *J. Memb. Sci.* **2005**, *267*, doi:10.1016/j.memsci.2005.06.004.
57. Wind, J. D.; Staudt-Bickel, C.; Paul, D. R.; Koros, W. J. Solid-State Covalent Cross-Linking of Polyimide Membranes for Carbon Dioxide Plasticization Reduction. *Macromolecules* **2003**, *36*, 1882–1888, doi:10.1021/ma025938m.
58. Kim, J. H.; Koros, W. J.; Paul, D. R. Physical aging of thin 6FDA-based polyimide membranes containing carboxyl acid groups. Part II. Optical properties. *Polymer (Guildf).* **2006**, *47*, 3104–3111.
59. Kim, J. H.; Koros, W. J.; Paul, D. R. Effects of CO2 exposure and physical aging on the gas permeability of thin 6FDA-based polyimide membranes. Part 2. with crosslinking. *J. Memb. Sci.* **2006**, *282*, doi:10.1016/j.memsci.2006.05.003.
60. Askari, M. CO2/CH4 Sorption Behavior of Glassy Polymeric Membranes Based on Dual Mode Sorption Model. *Bull. la Société R. des Sci. Liège* **2017**, *50*, 139–156, doi:10.25518/0037-9565.6628.
61. Martin-Gil, V.; Dujardin, W.; Sysel, P.; Koeckelberghs, G.; Vankelecom, I. F. J.; Fila, V. Effect of benzoic acid content on aging of 6FDA copolyimides based thin film composite (TFC) membranes in CO2/CH4 environment. *Sep. Purif. Technol.* **2019**, *210*, 616–626, doi:10.1016/j.seppur.2018.08.047.
62. Huertas, R. M.; Tena, A.; Lozano, A. E.; de Abajo, J.; de la Campa, J. G.; Maya, E. M. Thermal degradation of crosslinked copolyimide membranes to obtain productive gas separation membranes. *Polym. Degrad. Stab.* **2013**, *98*, 743–750, doi:10.1016/j.polymdegradstab.2012.12.017.
63. Hess, S.; Staudt, C. Variation of esterfication conditions to optimize solid-state crosslinking reaction of DABA-containing copolyimide membranes for gas separations. *Desalination* **2007**, *217*, doi:10.1016/j.desal.2007.01.011.
64. Calle, M.; Lozano, A. E.; de Abajo, J.; de la Campa, J. G.; Álvarez, C. Design of gas separation membranes derived of rigid aromatic polyimides. 1. Polymers from diamines containing di-tert-butyl side groups. *J. Memb. Sci.* **2010**, *365*, 145–153, doi:10.1016/j.memsci.2010.08.051.

65. Álvarez, C.; Lozano, Á. E.; Juan-y-Seva, M.; de la Campa, J. G. Gas separation properties of aromatic polyimides with bulky groups. Comparison of experimental and simulated results. *J. Memb. Sci.* **2020**, *602*, 117959, doi:10.1016/j.memsci.2020.117959.
66. Eguchi, H.; Kim, D. J.; Koros, W. J. Chemically cross-linkable polyimide membranes for improved transport plasticization resistance for natural gas separation. *Polymer (Guildf).* **2015**, *58*, 121–129, doi:10.1016/j.polymer.2014.12.064.
67. Katarzynski, D.; Staudt-Bickel, C. Separation of multi component aromatic/aliphatic mixtures by pervaporation with copolyimide membranes. *Desalination* **2006**, *189*, doi:10.1016/j.desal.2005.06.015.
68. Liaw, D. J.; Liaw, B. Y. Synthesis and properties of polyimides derived from 1,4-bis(4-Aminophenoxy)2,5-di-tert-butylbenzene. *J. Polym. Sci. Part A Polym. Chem.* **1997**, *35*, doi:10.1002/(SICI)1099-0518(199706)35:8<1527::AID-POLA21>3.0.CO;2-8.
69. BIOVIA Dassault Systémes, Biovia Materials Studio, 2017R2, San Diego: Dassault Systèmes,. *Dassault Systèmes* 2017.
70. Adewole, J. K.; Ahmad, A. L.; Ismail, S.; Leo, C. P. Current challenges in membrane separation of CO2 from natural gas: A review. *Int. J. Greenh. Gas Control* **2013**, *17*, 46–65, doi:10.1016/j.ijggc.2013.04.012.
71. Muñoz, D. M.; de la Campa, J. G.; de Abajo, J.; Lozano, A. E. Experimental and Theoretical Study of an Improved Activated Polycondensation Method for Aromatic Polyimides. *Macromolecules* **2007**, *40*, 8225–8232, doi:10.1021/ma070842j.
72. Muñoz, D. M.; Calle, M.; de la Campa, J. G.; de Abajo, J.; Lozano, A. E. An Improved Method for Preparing Very High Molecular Weight Polyimides. *Macromolecules* **2009**, *42*, 5892–5894, doi:10.1021/ma9005268.
73. Maya, E. M.; García-Yoldi, I.; Lozano, A. E.; de la Campa, J. G.; de Abajo, J. Synthesis, Characterization, and Gas Separation Properties of Novel Copolyimides Containing Adamantyl Ester Pendant Groups. *Macromolecules* **2011**, *44*, 2780–2790, doi:10.1021/ma200093j.
74. Wieneke, J. U.; Staudt, C. Thermal stability of 6FDA-(co-)polyimides containing carboxylic acid groups. *Polym. Degrad. Stab.* **2010**, *95*, 684–693, doi:10.1016/j.polymdegradstab.2009.11.041.
75. Kratochvil, A. M.; Koros, W. J. Decarboxylation-Induced Cross-Linking of a Polyimide for Enhanced CO 2 Plasticization Resistance. *Macromolecules* **2008**, *41*, 7920–7927, doi:10.1021/ma801586f.
76. Qiu, W.; Chen, C. C.; Kincer, M. R.; Koros, W. J. Thermal analysis and its application in evaluation of fluorinated polyimide membranes for gas separation. *Polymer (Guildf).* **2011**, *52*, 4073–4082, doi:10.1016/j.polymer.2011.07.002.
77. Konietzny, R.; Barth, C.; Harms, S.; Raetzke, K.; Koelsch, P.; Staudt, C. Structural investigations and swelling behavior of 6FDA copolyimide thin films. *Polym. Int.* **2011**, *60*, doi:10.1002/pi.3123.
78. Hibshman, C.; Cornelius, C. .; Marand, E. The gas separation effects of annealing polyimide–organosilicate hybrid membranes. *J. Memb. Sci.* **2003**, *211*, 25–40, doi:10.1016/S0376-7388(02)00306-X.
79. Robeson, L. M. Correlation of separation factor versus permeability for polymeric membranes. *J. Memb. Sci.* **1991**, *62*, 165–185, doi:10.1016/0376-7388(91)80060-J.
80. Robeson, L. M. The upper bound revisited. *J. Memb. Sci.* **2008**, *320*, 390–400, doi:10.1016/j.memsci.2008.04.030.
81. Minelli, M.; Oradei, S.; Fiorini, M.; Sarti, G. C. CO2 plasticization effect on glassy polymeric membranes. *Polymer (Guildf).* **2019**, *163*, 29–35, doi:10.1016/j.polymer.2018.12.043.